

~~CONFIDENTIAL~~

Copy 5
RM L53L15

NACA RM L53L15



RESEARCH MEMORANDUM

INVESTIGATION OF A PULSE-JET-POWERED HELICOPTER ROTOR ON
THE LANGLEY HELICOPTER TEST TOWER

By Edward J. Radin and Paul J. Carpenter

Langley Aeronautical Laboratory
Langley Field, Va.

CLASSIFICATION CANCELLED

Authority NACA R7 3145 Date 10/14/53

By 2177A 10/26/53 See _____

CLASSIFIED DOCUMENT

This material contains information affecting the National Defense of the United States within the meaning of the espionage laws, Title 18, U.S.C., Secs. 793 and 794, the transmission or revelation of which in any manner to an unauthorized person is prohibited by law.

**NATIONAL ADVISORY COMMITTEE COPY
FOR AERONAUTICS**

WASHINGTON
February 8, 1954

FEB 15 1954

LANGLEY AERONAUTICAL LABORATORY
LIBRARY, NACA
LANGLEY FIELD, VIRGINIA

~~CONFIDENTIAL~~

NATIONAL ADVISORY COMMITTEE FOR AERONAUTICS

RESEARCH MEMORANDUM

INVESTIGATION OF A PULSE-JET-POWERED HELICOPTER ROTOR ON

THE LANGLEY HELICOPTER TEST TOWER

By Edward J. Radin and Paul J. Carpenter


SUMMARY

A helicopter rotor powered by pulse-jet engines located at the rotor-blade tips has been investigated on the Langley helicopter test tower. The basic hovering characteristics of the rotor and the propulsive characteristics of the pulse-jet engine were obtained over a range of engine speeds from 260 to 422 fps with the engines rigidly fixed to the blade tips and with the engines free to pivot in pitch. The rotor was also investigated in the power-off condition (engines fixed and pivoted) and with the engines removed. Additional measurements included the determination of the effect of inlet blockage on the power-off drag of the jet engines and the determination of noise intensity in the vicinity of the operating engines.

INTRODUCTION

The helicopter powered by jet engines mounted at the rotor tips is of interest for short-range applications because of mechanical simplicity and high ratio of payload to gross weight. Inasmuch as the overall performance of such helicopters is closely dependent on the aerodynamic and propulsive characteristics of the engine, a study of tip jet-rotor systems has been undertaken by the National Advisory Committee for Aeronautics. The first step in the study was the investigation of ram-jet powered rotors on the Langley helicopter test tower, references 1 and 2. The present paper reports an investigation of a pulse-jet-powered rotor on the same facility. The pulse-jet engine was developed specifically for helicopter use by a private contractor. The rotor diameter and solidity were selected to absorb the engine power efficiently at low tip speeds where the pulse-jet operates efficiently.

This investigation included the determination of the engine drag as a function of tip speed and blade pitch angle in the power-off condition and the determination of the propulsive thrust of the engine and the rotor lift as a function of fuel-flow rate for a range of rotor tip speeds. The



cold drag of the engines was determined with the inlet open and with the inlet completely blocked and with the engines rigidly attached and free to pivot in pitch. Limited measurements of the noise level and information on valve life were also obtained.

SYMBOLS

R	blade radius (measured to inboard side of jet engine), ft
T	rotor thrust, lb
Q	rotor torque, ft-lb
ρ	air density, slugs/cu ft
Ω	rotor angular velocity, radians/sec
C_T	rotor thrust coefficient, $T/\pi R^2 \rho (\Omega R)^2$
C_Q	rotor torque coefficient, $Q/\pi R^2 \rho (\Omega R)^2 R$
A_j	maximum external cross-sectional area of jet engine (0.483 sq ft)
D_j	total (internal, external, and interference) power-off drag of jet engine, lb
V	velocity of pulse-jet engine, fps
V_c	corrected velocity of pulse-jet engine, $V/\sqrt{\theta}$, fps
V_t	corrected rotor blade tip speed (at radius R), fps
g	acceleration due to gravity, 32.2 ft/sec ²
ΔF	total change in force at blade tip from power-off to power-on conditions, lb
D_R	drag corresponding to torque of rotor without engine at same C_T and tip speed, lb
$D_{t_{cold}}$	power-off drag of engine at 0° angle of attack, lb
$\Delta D_{t_{cold}}$	increment of engine drag due to angle of attack, lb

K_1	thrust required to accelerate fuel to engine velocity, lb
K_2	mutual interference drag between engine and blade at 0° angle of attack, lb
ΔK_2	increment of mutual interference drag between engine and blade due to angle of attack, lb
C_{D_j}	total (internal, external, and interference) power-off drag coefficient, $D_j / \frac{1}{2} \rho V^2 A_j$
F_p	propulsive thrust of jet engine, $D_R + \Delta D_{t_{cold}} + \Delta K_2 + K_1$, lb
W_f	fuel-flow rate, lb/hr
W_{fc}	corrected fuel-flow rate, $W_f / \delta \sqrt{\theta}$, lb/hr
δ	ratio of ambient pressure to standard NACA sea-level pressure
θ	ratio of absolute static temperature to standard NACA sea-level absolute temperature

APPARATUS

The Langley helicopter test tower is described in reference 3, except for the fuel and ignition systems which are described in reference 1.

Rotor

The rotor was a two-bladed type with drag hinges and offset flapping hinges; however, the drag hinges were locked in the 0° lag angle for the present investigation. The blades were plywood covered, had a tubular steel main spar and NACA 23015 airfoil sections. The radius of the rotor was 18.54 feet to the blade tip and 18.84 feet to the center line of the jet engines. The blade had a 27.3-inch chord between the 21.6- and 71.5-percent-radius stations with lineal taper to a chord of 23.7 inches at the tip. The solidity (ratio of blade area to disk area) of the rotor was 0.073. Inasmuch as the torsional stiffness of the blades was approximately 4,460 in-lb/deg of twist, the blade twist due to pitching moments of the engine was considered negligible. A general view of the pulse-jet rotor mounted on the helicopter tower is shown in figure 1.

The rotor was tested in two configurations, first with the jet engines rigidly attached to the blade spar so that the jet shell was horizontal when the blade pitch was zero and secondly with the jet engines free to pivot in pitch. For the latter condition, as shown in figure 1, a stabilizer (62.8 sq in. of area) was attached to the rear outboard side of the jet engine, so that the engine was trimmed to approximately 0° angle of attack throughout the range of blade pitch angles. The blade extended to within approximately $1/16$ inch of the pulse-jet-engine shell in both configurations. This gap was left to provide freedom of movement when the jet engines were free to pivot. The blade intersected the pulse-jet shell at approximately a 90° angle and no fillets were provided. The center of gravity of the jet engine for the rigidly attached case was located on the axis of the main blade spar.

Engine

The pulse jet used for the investigation had an operating frequency of about 100 cps, weighed 36 pounds, and was 49.7 inches in length with a maximum diameter of 9.4 inches. It should be pointed out that in helicopter applications, the pulse-jet performance, compared to those used in nonrotating applications, has been compromised by decreasing the tail-pipe length as much as possible both to reduce engine weight and to alleviate engine deformation under centrifugal loads. A sketch of the pulse-jet engine is shown in figure 2.

The conventional-flapper-type valve box, a photograph of which is shown in figure 3(a), was used in conjunction with the engine. Figure 3(b) shows the arrangement of the moving parts of the valve box which consisted of a sandwich of one (0.005-inch-thick) phosphor bronze strip between two (0.006-inch-thick) blued-steel strips. These strips were 1 inch wide by 6 inches long. The spring constant of the valves was 20 pounds per inch deflection of the valve tips.

The fuel-injection system consisted of four fuel-spray nozzles located immediately to the rear of the valve box and spraying toward the center of the engine. The fuel nozzles were rated at 15.0 gallons per hour at 100 lb/sq in. and had a 60° spray cone angle.

METHODS AND ACCURACY

Test Conditions and Rotor Characteristics

All tests on the Langley helicopter test tower were made with ambient wind velocities less than 5 miles per hour and all measurements were obtained under steady-state operating conditions. The test procedure was

to establish a constant rotor tip speed by varying either the tower drive-motor power or the pulse-jet-engine thrust as rotor thrust was varied through the desired range by changing the blade-pitch angle. The tower thrust and torque tares for both power-off and power-on operating conditions were negligible.

The performance of the rotor with and without the "cold" (power-off) jet engines attached was determined directly from the conventional tower drive-shaft measurements of thrust and torque. From these measurements, curves of rotor-thrust coefficient against torque coefficient were plotted. The cold drag of the jet engines for various speeds and angles of attack was determined from the differences in rotor torque coefficient with and without engines at given rotor tip speeds and thrust coefficients. The cold drag of the engine, so defined, includes a small increment corresponding to the total interference drag between the rotor and the tip engines.

For the power-on engine-operating condition, the rotor thrust again was determined directly from the tower shaft measurements. The propulsive thrust of the engine, however, had to be calculated indirectly by the method outlined in the appendix of reference 1. This method assumed, in essence, that the torque overcome by the jet engines was equal to the torque of the basic rotor without tip engines at the same rotor thrust coefficient plus the torque chargeable to fuel pumping within the blades plus an increment in torque corresponding to the increases, due to angle of attack, of engine cold drag and of mutual interference drag between the rotor and the tip engines. In this procedure the force corresponding to the measured torque required to drive the rotor with engines attached in the power-off condition is first calculated. This force plus the engine thrust required for fuel pumping is equivalent to the net change in force at the blade tip from engine power-off to power-on conditions and can be written as:

$$\Delta F = K_1 + D_R + D_{t_{cold}} + K_2 + \Delta D_{t_{cold}} + \Delta K_2$$

Subtracting out the measured power-off engine drag at 0° angle of attack $D_{t_{cold}} + K_2$ gives the engine propulsive thrust which is

$$F_p = K_1 + D_R + \Delta D_{t_{cold}} + \Delta K_2$$

Contamination effects (increase in temperature of the air through which the engine passes caused by the exhaust of the previous engine) were not determined and corrections for these effects have not been applied. Tests of a ram-jet rotor with similar blade radius and fuel-flow rates

(ref. 2) indicate that contamination decreased the engine thrust by about 3 percent at a tip speed of about 680 fps. The decrease would be expected to be even less than this value for the pulse-jet rotor because of higher rotor disk loading (higher induced velocity) and much lower tip speeds.

The effect of centrifugal distortion of the fuel spray pattern also was not determined. This effect is probably small, however, because the centrifugal accelerations are small (about 400g) and previous investigations (ref. 2) have indicated little effect on ram-jet engine performance at centrifugal accelerations under 400g.

The power-on performance has been reduced to that which would have been obtained under standard conditions by the method outlined in reference 4.

In order to avoid overheating the pulse-jet engines during starting, the rotor was brought up to a tip speed of about 200 fps with the conventional tower drive motor. At this speed, fuel was injected into one pulse-jet engine and as soon as the engine was resonating properly, the tower drive was disengaged. Fuel was then injected into the other engine and test data were obtained as soon as both engines were at steady-state conditions.

Engine Static-Thrust Performance

Static-thrust performance of the engine at various fuel-flow rates was obtained on a static-thrust stand which incorporated a thrust balance and a fuel-flow meter. An airstream at a velocity of about 200 fps was directed at the inlet of the engine. As soon as the engine began resonating, the air supply was removed and the static performance of the pulse-jet engine was determined.

Estimated Accuracies

The estimated accuracies of the basic quantities measured in the tests are as follows: rotor thrust, ± 15 pounds; rotor torque, ± 20 foot-pounds; blade root pitch angle, $\pm 0.1^\circ$; fuel-flow rate, ± 10 pounds per hour; and rotor angular speed, ± 1 rpm. The overall accuracy of the plotted results is believed to be ± 3 percent.

RESULTS AND DISCUSSION

Characteristics of Rotor and Rotor With Engines Inoperative

The rotor characteristics are presented in figure 4 as a plot of thrust coefficient against torque coefficient. The curve for the rotor alone was determined for a blade tip speed of 370 fps and would be expected to remain the same for tip speeds up to about 500 fps. The characteristics of the rotor with the inoperative engines rigidly fixed and with the inlet open are also shown. An estimated curve obtained by extrapolating the measured data is presented for a speed of 260 fps inasmuch as this information was needed to determine the propulsive thrust plus power-off drag. An inspection of the curves indicates that the torque increment due to adding the engines to the blades increases with tip speed and to a lesser extent with increases in rotor thrust or blade-pitch angle. Jet-engine drag coefficients calculated from these torque increments will be presented later.

Inasmuch as there was some increase in power-off drag coefficient at high rotor thrust coefficients (high blade pitch angles) it was believed that some reduction in pulse jet drag, which would improve the autorotative characteristics of the rotor, could be realized by allowing the engine to pivot and thus align itself with the airstream regardless of blade-pitch angles. A comparison of the power-off rotor torque coefficients for various rotor thrust coefficients at a tip speed of 321 fps for the rigidly attached and pivoted engine installations is shown in figure 5. These curves indicate that some small reduction was realized at the higher blade angles of attack. The power-off drag decrease was not as large as expected; a 30-percent increase in jet-engine drag above that obtained at zero rotor thrust coefficient with both blade and jet engine set at 0° angle of attack remained at a rotor thrust coefficient of 0.005. The increased drag is attributed to unfavorable interference when the pulse jet is not aligned with the blade chord, to loss of end-plate effect, and to the drag of the stabilizing tab. The calculated drag and lift attributed to the stabilizer for a rotor tip speed of 420 fps and 1° angle of attack were 0.8 and 6 pounds, respectively. These values of drag and lift could not be accurately determined experimentally inasmuch as they are of the same magnitude as the test accuracy. A further decrease in jet-engine drag possibly could have been realized by the use of a suitable flexible fairing between the blade tip and the engine. Despite the small gain indicated, pivoting may be desirable to reduce the cyclic control forces in forward flight.

Engine Characteristics

Power-off.- The power-off total drag coefficients of the pulse-jet engine rigidly fixed to the blade as determined in the tower tests for the conditions of 0° angle of attack of the rotor blade and 0° engine incidence are presented in figure 6 as a function of speed for the engine with the inlet open and with the inlet completely blocked. The values of drag contain the aforementioned interference drag between the blade and engine. The engine drag coefficient increased rapidly from 0.18 at 270 fps to 0.30 at 400 fps because the valves opened more and more as the dynamic pressure was increased, allowing more air to pass through the engine. With the inlet fully blocked, the drag coefficient was constant (0.15) over the speed range. A decrease in engine-drag coefficient of about 17 percent at 270 fps and 50 percent at 400 fps is shown for the fully blocked inlet. This reduction clearly indicates the desirability of blocking off the air flow through the engine in the event of power failure.

The variation with blade pitch angle of the pulse-jet engine power-off drag coefficient with inlet open and with the engine rigidly attached to the blade is presented in figure 7 for a range of speeds from 273 to 403 fps. These drag coefficients contain mutual-interference effects of the blade-engine combination and any effects of the engine on rotor efficiency. The power-off drag of the engine was approximately 24 percent greater at 6° angle of attack than at 0° for a speed of 273 fps. As has been previously pointed out, some decrease in drag can be achieved by pivoting the engine, and a much larger decrease can be obtained by blocking off the inlet air.

Power-on.- The variation of pulse-jet propulsive thrust plus total power-off drag is shown in figure 8 as a function of fuel-flow rate for various rotor speeds with the engine fixed rigidly to the blade tips. The propulsive thrust plus power-off drag is the quantity denoted by the symbol ΔF in the previous description of the method of data reduction.

The corrected engine velocities V_c of figure 8 were 368, 319, and 260 fps, whereas, the uncorrected velocities were 376, 326, and 268 fps, respectively. The determination of the power-off drag for the curve of 260 fps involved a slight extrapolation of the drag data from 273 to 260 fps. The range of blade-root pitch angles for the power-on investigation was from 0° to approximately 12° . A curve of the static-thrust characteristics of the engine is also given on figure 8.

The results given in figure 8 are replotted in figure 9 in terms of the estimated propulsive thrust against fuel-flow rate. It is noted that the curve for 422 fps was obtained by an appreciable extrapolation of drag data. The extrapolation does not present a very serious problem,

however, inasmuch as it is used only to determine the increment in drag due to angle of attack.

A primary characteristic of the pulse-jet engine is a decrease in propulsive thrust with increase in speed. This effect is clearly shown in figure 9. For example, at a fuel rate of 240 pounds per hour, the propulsive thrust decreased from 78 pounds to 30 pounds over a speed range of 0 to 422 fps. The decrease is usually attributed to a combination of several factors: namely, failure of inlet valves to close completely at higher speeds, higher combustion-chamber velocities, and decrease in tail-pipe charging. All of these factors tend to decrease the combustion-chamber pressure ratio.

The point at which the engine failed to resonate because of an increase in fuel rate (rich blowout) is shown in figure 9 for all speeds except for 422 fps. At 422 fps, the oil canning caused by intermittent stopping of the inlet air flow resulted in repeated fatigue failures in the inlet cowling. Consequently, only a limited amount of data could be obtained and neither the maximum-thrust point nor the rich-blowout point was obtained.

The maximum thrust at all forward speeds was obtained at the rich-blowout point. These maximum values therefore cannot be utilized for design purposes inasmuch as some margin of safety must be provided to avoid sudden loss of power. This rich blowout may not be too serious if the machine has sufficient altitude because it was always possible to restart the engines on the test tower by merely decreasing the fuel-flow rate as long as the tip speed was not permitted to drop below 200 fps.

The region of lean blowout is shown on the static-thrust curve. Lean blowout was not obtained in the whirling conditions.

The minimum specific fuel consumption in pounds of fuel per hour per horsepower and the propulsive thrusts at these minimum specific fuel consumptions are shown in figure 10 as a function of velocity. The curves show a decrease in specific fuel consumption from the lowest operating speed of 260 fps to about 340 fps, at which point the specific fuel consumption started to increase. No data are shown for an engine velocity of 422 fps since the minimum specific fuel consumption probably was not reached due to cowling inlet failure. The minimum specific fuel consumption of 6.6 pounds of fuel per hour per horsepower for the helicopter-type pulse jet investigated is higher than that for pulse-jet engines used in nonrotating applications and is higher than the values sometimes assumed in theoretical analyses of helicopter pulse-jet propulsion systems.

The velocity at which the minimum specific fuel consumption was attained and the velocity at which the engine thrust for minimum specific fuel consumption drops off indicates that the optimum tip speeds for

pulse-jet-propelled rotors using engines similar to the one investigated will be approximately 320 to 360 fps. Similar data for the ram-jet-propelled rotor (ref. 2) show, in contrast, that the optimum ram-jet-engine operating conditions occur at maximum tip speeds obtainable (680 fps or greater) as limited by structural considerations. Thus, the forward speed of a pulse-jet-powered helicopter would appear to be more limited than that of the ram-jet-powered types because of the relatively low tip speed at which the pulse-jet engine operates most efficiently.

Power-On Characteristics of Engine-Rotor Combination

The hovering characteristics of the pulse-jet rotor with the engines rigidly attached are presented in figure 11 in terms of the variation of corrected rotor thrust with corrected total (2 pulse jets) fuel consumption for corrected rotor blade tip speeds from 256 to 415 fps. The data obtained with the pulse jets pivoted gave identical rotor-thrust and fuel-consumption curves. From the comparison of the power-off drag of the rigidly attached and pivoted engines in figure 5, some small difference would be expected. This difference, however, was not realized.

The rotor performance was penalized somewhat in these particular tests due to roughness of the blade surface. The drag coefficient at zero lift was about 0.012 as compared with 0.008 realized on semismooth airfoil sections of the same shape and construction.

The maximum ratio of rotor thrust to fuel consumption was obtained at the lowest speed tested, because the solidity was 0.073, a value which was nearly optimum for hovering performance at tip speeds of 260 fps but which provided considerable excess blade area for the power available at higher speeds. For maximum values of the ratio of rotor thrust to fuel consumption, the rotor solidity must be such as to give maximum rotor efficiency at the tip speed corresponding to the minimum engine specific fuel consumption. If a lower solidity had been used in the present investigation, the curves for a tip speed of 314 and 362 fps probably would have yielded higher maximum ratios of thrust to fuel consumption than the present curve for a tip speed of 256 fps. From the foregoing, and as discussed in references 1 and 5, it is apparent that the matching of the rotor and engine characteristics is of major importance.

Operational Characteristics

Noise intensity.- The noise intensity of the pulse-jet engine was measured at three arbitrary stations in the vicinity of the test tower. A noise level of about 135 decibels was measured at a station approximately 3 feet above the rotor hub at the center of rotation for the maximum power condition. Approximately 132 decibels were measured for the same

condition at a station 40 feet below the rotor and 95 feet from the center of rotation. At a point 2 feet above the path of the blade tips, the maximum noise level was in the region of 140 decibels when the engine passed nearest to the recording instruments.

Valve life.- The life of the valves depended mainly upon the thrust delivered by the engine. At maximum thrust, the valve life was approximately 20 minutes to 1 hour, whereas 8 to 10 hours of operation could be expected by operating at 75 percent of maximum thrust. The original valve seats were painted with several coats of a synthetic rubber. This coating tended to harden and erode rapidly under maximum-thrust conditions. The valve seats were then recoated with a special high-temperature rubber which did not erode or harden (Dow-Corning 160 rubber and Dow-Corning 50-c primer). This coating nearly doubled the valve life at approximately 75 percent engine thrust; however, valve life remained about the same for the maximum-thrust case.

CONCLUSIONS

The basic hovering characteristics of a pulse-jet-powered helicopter rotor and the power-off drag and propulsive characteristics of the pulse-jet engine have been determined on the Langley helicopter test tower. The more pertinent findings of this investigation are as follows:

1. The power-off drag coefficient of the pulse-jet engine increased from 0.18 to 0.30 as the speed increased from 270 to 400 fps. This increase was caused by an increase in internal drag with an increase in speed.
2. The power-off drag coefficient of the engine was reduced to 0.15 over the entire speed range investigated by blocking the inlet.
3. A minimum specific fuel consumption of 6.6 pounds of fuel per hour per horsepower was obtained for the speed range of 320 to 360 fps.
4. The noise level of the pulse-jet engine at maximum thrust was about 135 decibels at a station on the center of rotation and 3 feet above the hub.
5. The power-on performance of the pulse-jet-powered rotor was the same for the engine-fixed and engine-pivoted conditions. Little difference in power-off engine drag was noted for the two conditions.

Langley Aeronautical Laboratory,
National Advisory Committee for Aeronautics,
Langley Field, Va., November 27, 1953.

REFERENCES

1. Carpenter, Paul J., and Radin, Edward J.: Investigation of a Ram-Jet-Powered Helicopter Rotor on the Langley Helicopter Test Tower. NACA RM L53D02, 1953.
2. Radin, Edward J., and Carpenter, Paul J.: Comparison of the Performance of a Helicopter-Type Ram-Jet Engine Under Various Centrifugal Loadings. NACA RM L53H18a, 1953.
3. Carpenter, Paul J.: Effect of Wind Velocity on Performance of Helicopter Rotors As Investigated With The Langley Helicopter Apparatus. NACA TN 1698, 1948.
4. Sanders, Newell D.: Performance Parameters for Jet-Propulsion Engines. NACA TN 1106, 1946.
5. Gustafson, F. B., and Gessow, Alfred: Effect of Rotor-Tip Speed on Helicopter Hovering Performance and Maximum Forward Speed. NACA WR L-97, 1946. (Formerly NACA ARR L6A16.)



L-72051

Figure 1.- View of the pulse-jet powered helicopter rotor mounted on the helicopter test tower (engines free to pivot).

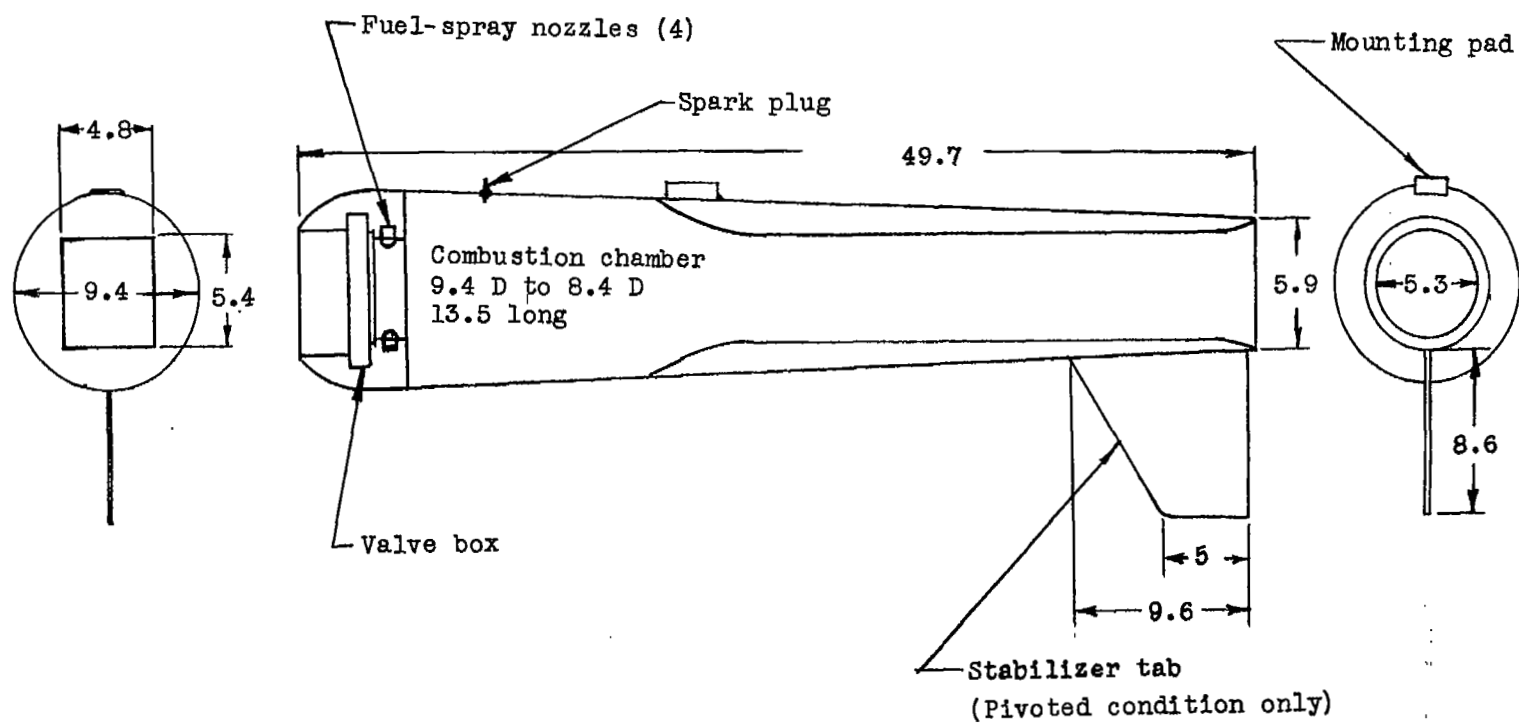
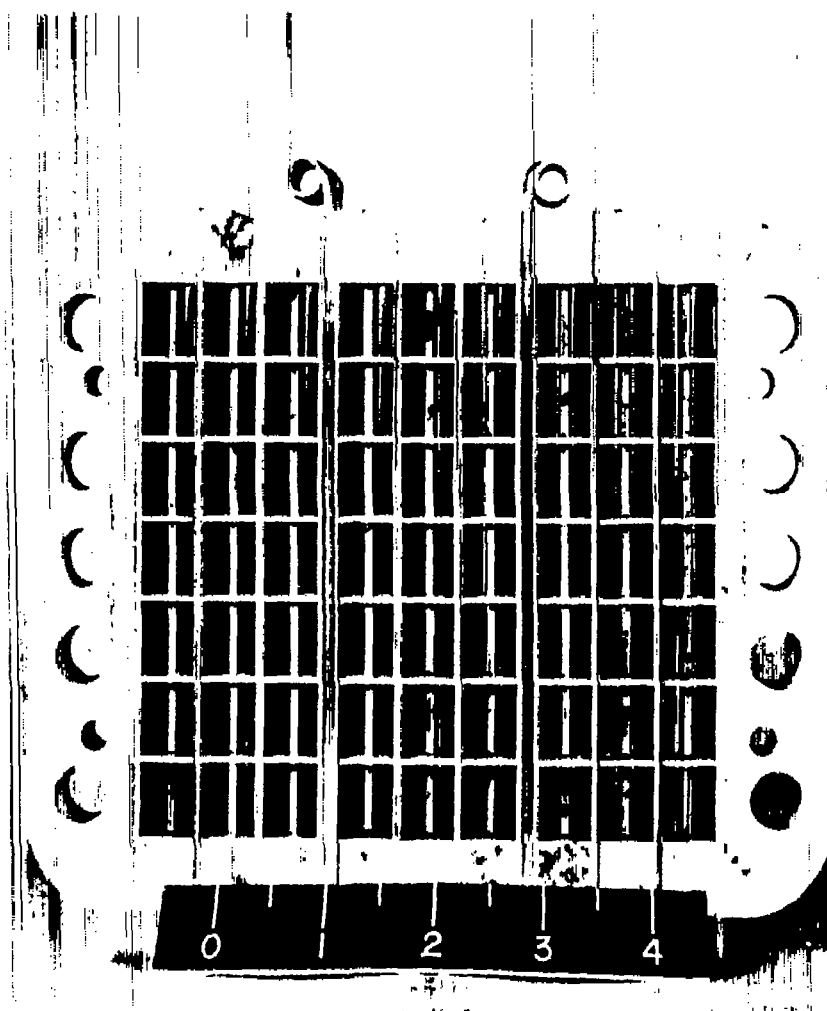
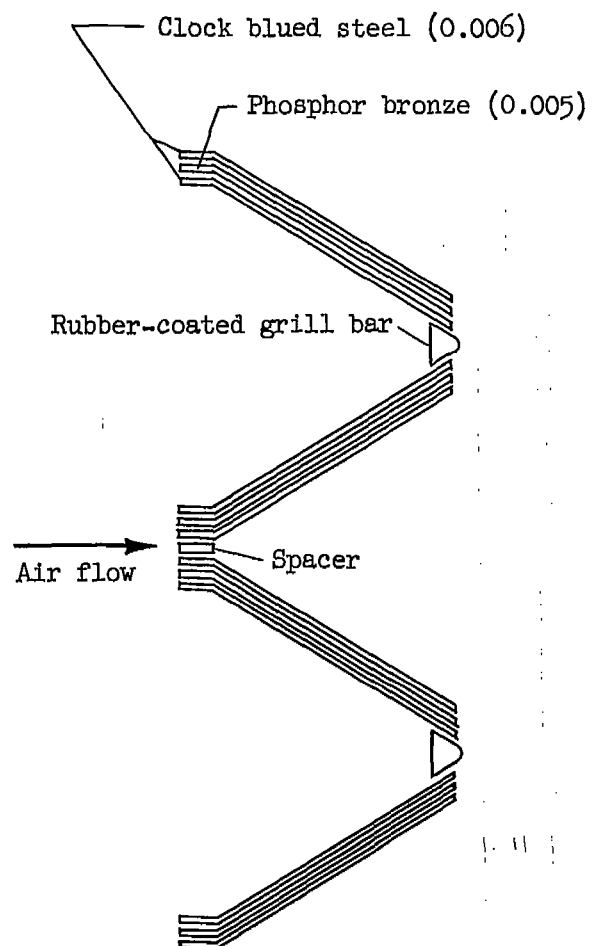


Figure 2.- Sketch of the pulse-jet engine. All dimensions are in inches.



(a) Front view.



(b) Valve detail.

L-80325.1

Figure 3.- Pulse-jet engine flapper-type valve box.

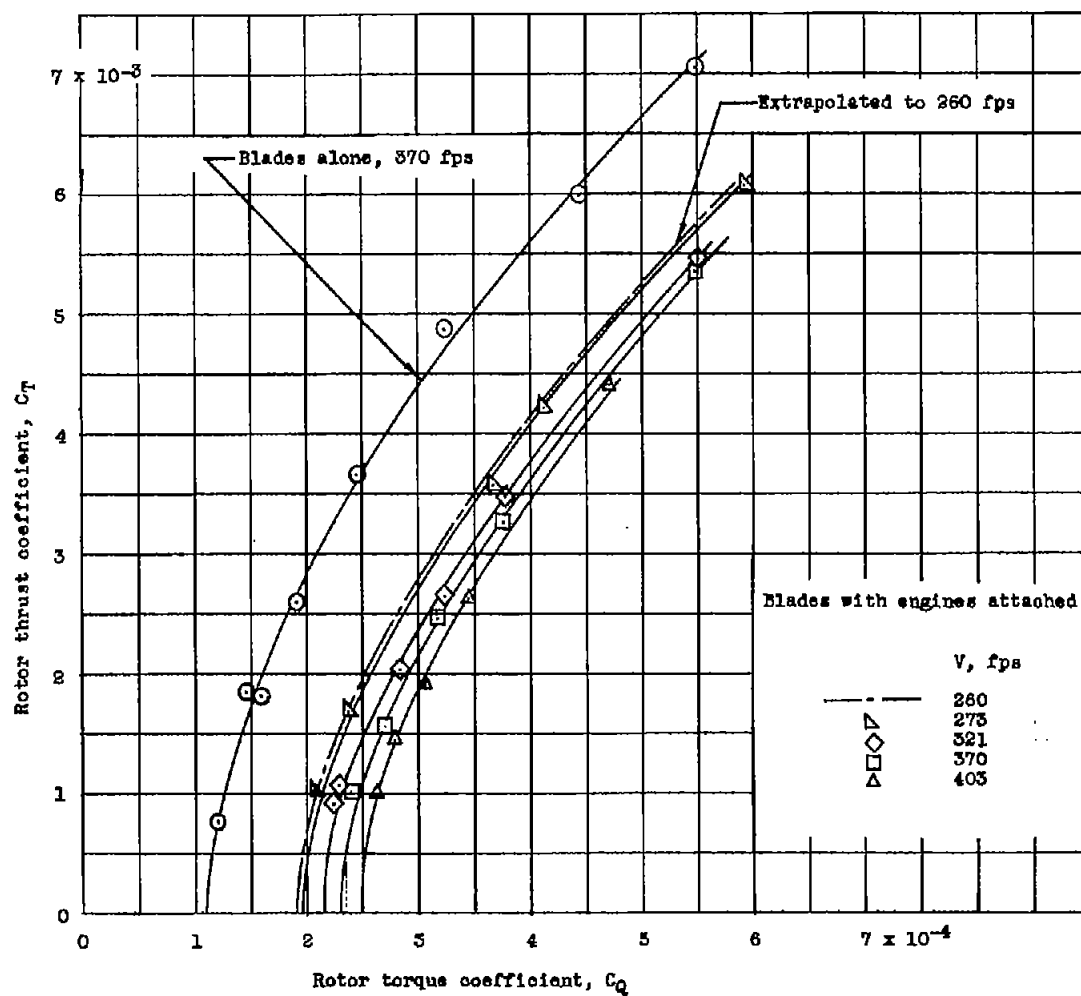


Figure 4.- Rotor thrust coefficient against rotor torque coefficient for the blades alone and for the blades with pulse-jet engines rigidly attached, power-off, inlets open.

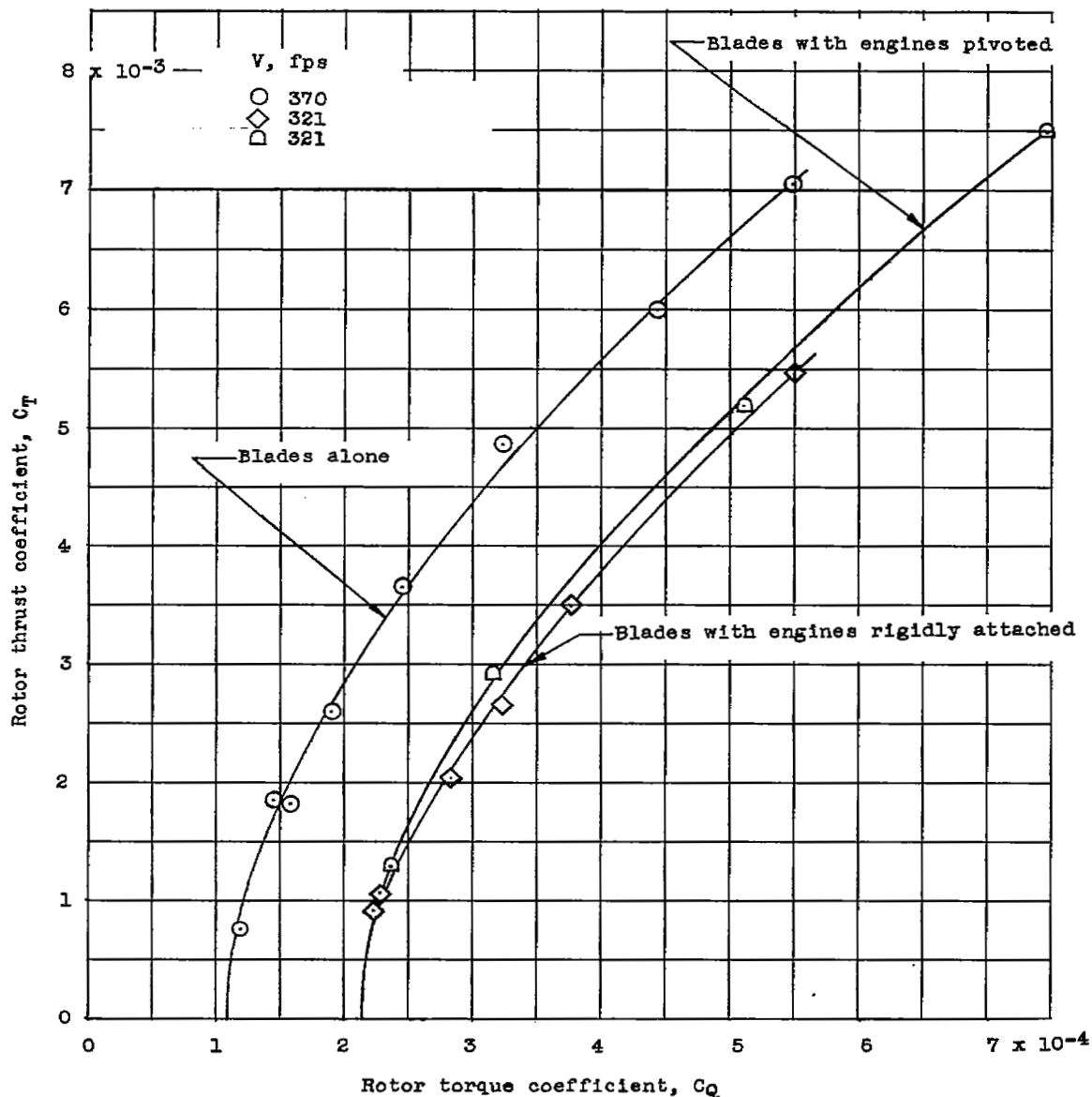


Figure 5.- Rotor thrust coefficient against rotor torque coefficient for the blades alone, for the blades with engines rigidly attached, and for the blades with engines pivoted, power-off, inlets open.

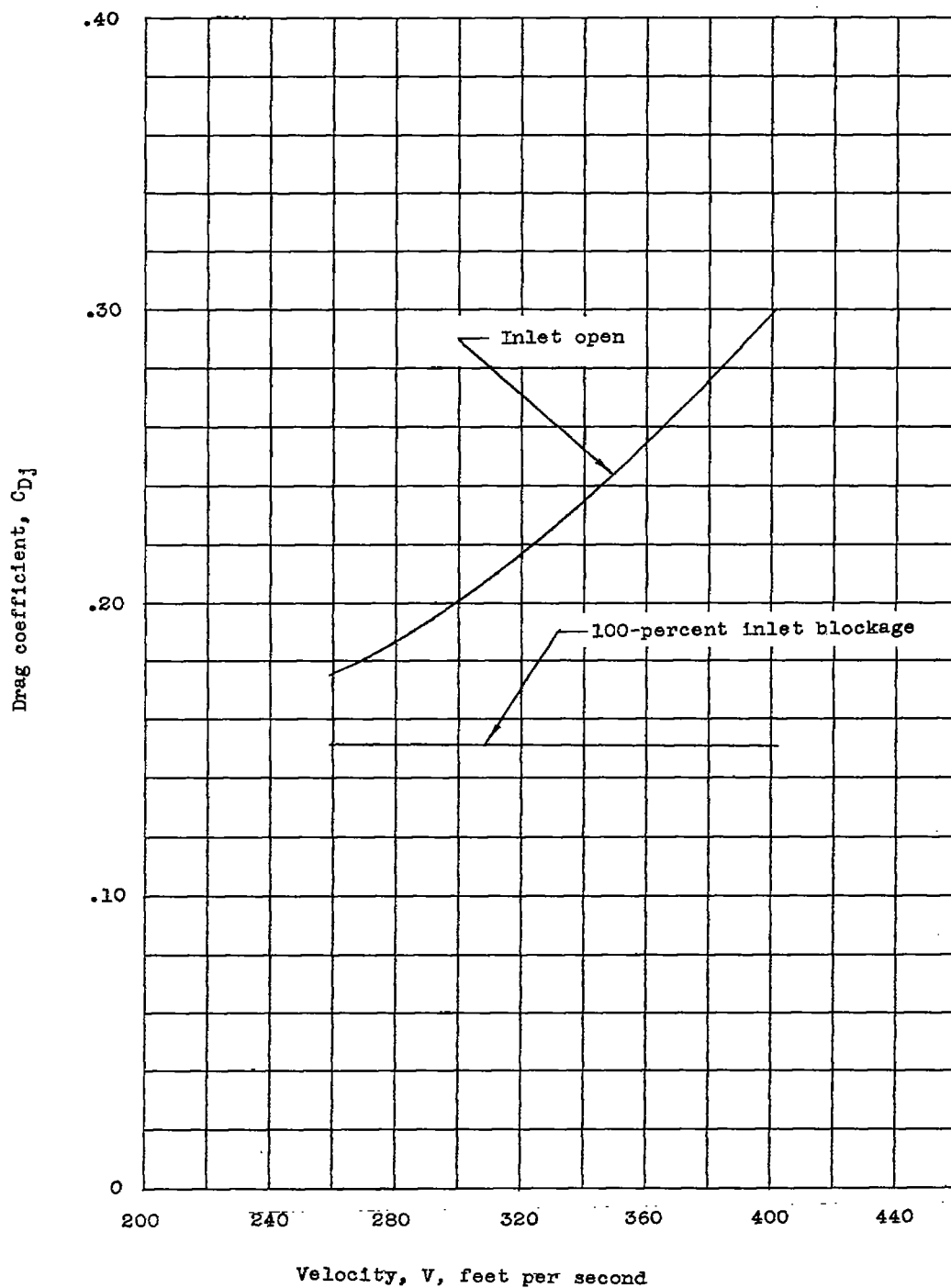


Figure 6.- Pulse-jet engine power-off drag coefficient as a function of velocity at 0° angle of attack and 0° engine incidence. Engine rigidly attached.

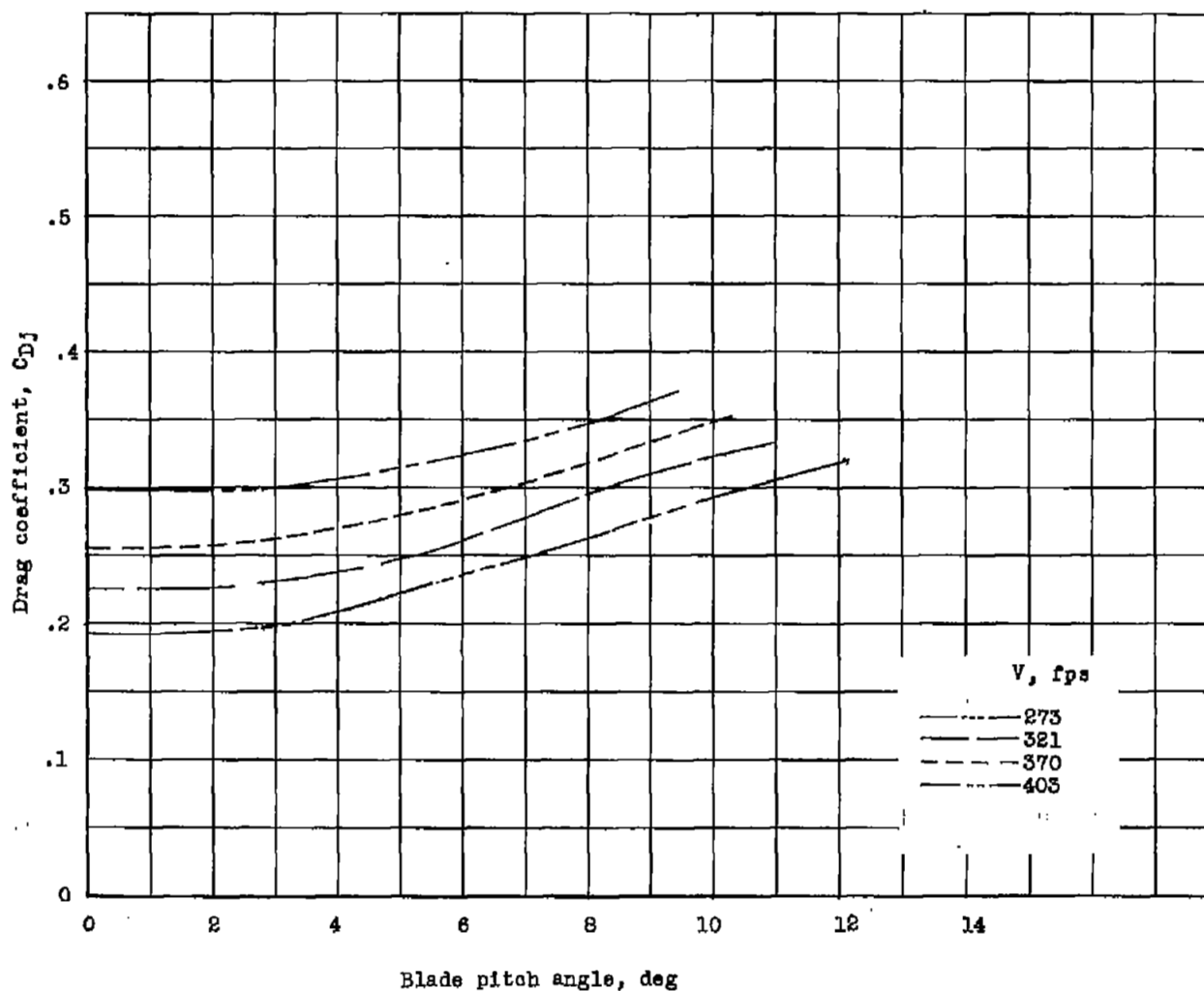


Figure 7.- Pulse-jet engine power-off drag as a function of blade pitch angle for a range of speeds from 273 to 403 fps. Engine rigidly attached and inlets open.

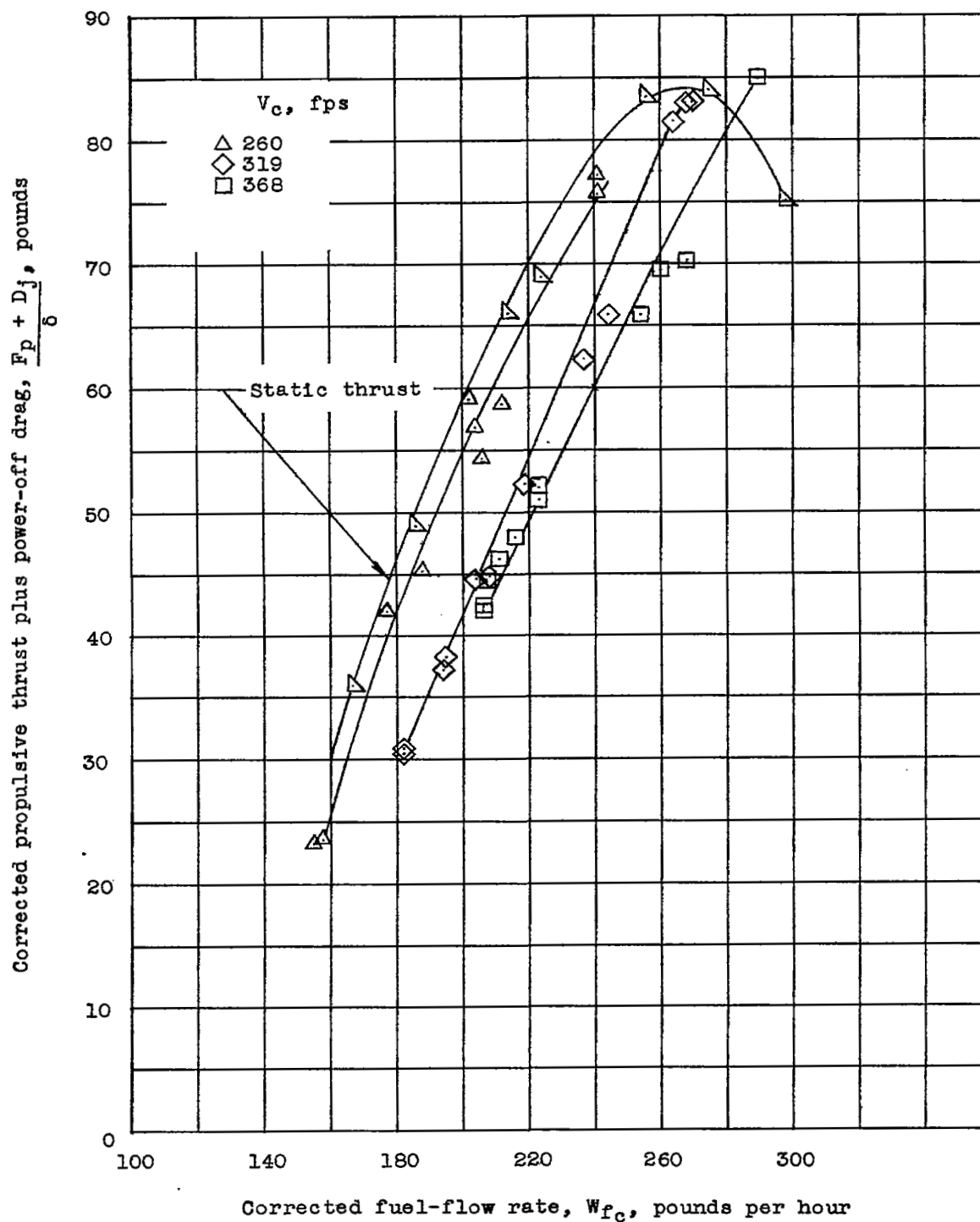


Figure 8.- Corrected pulse-jet propulsive thrust plus power-off drag against corrected fuel consumption for one engine. Engine rigidly attached.

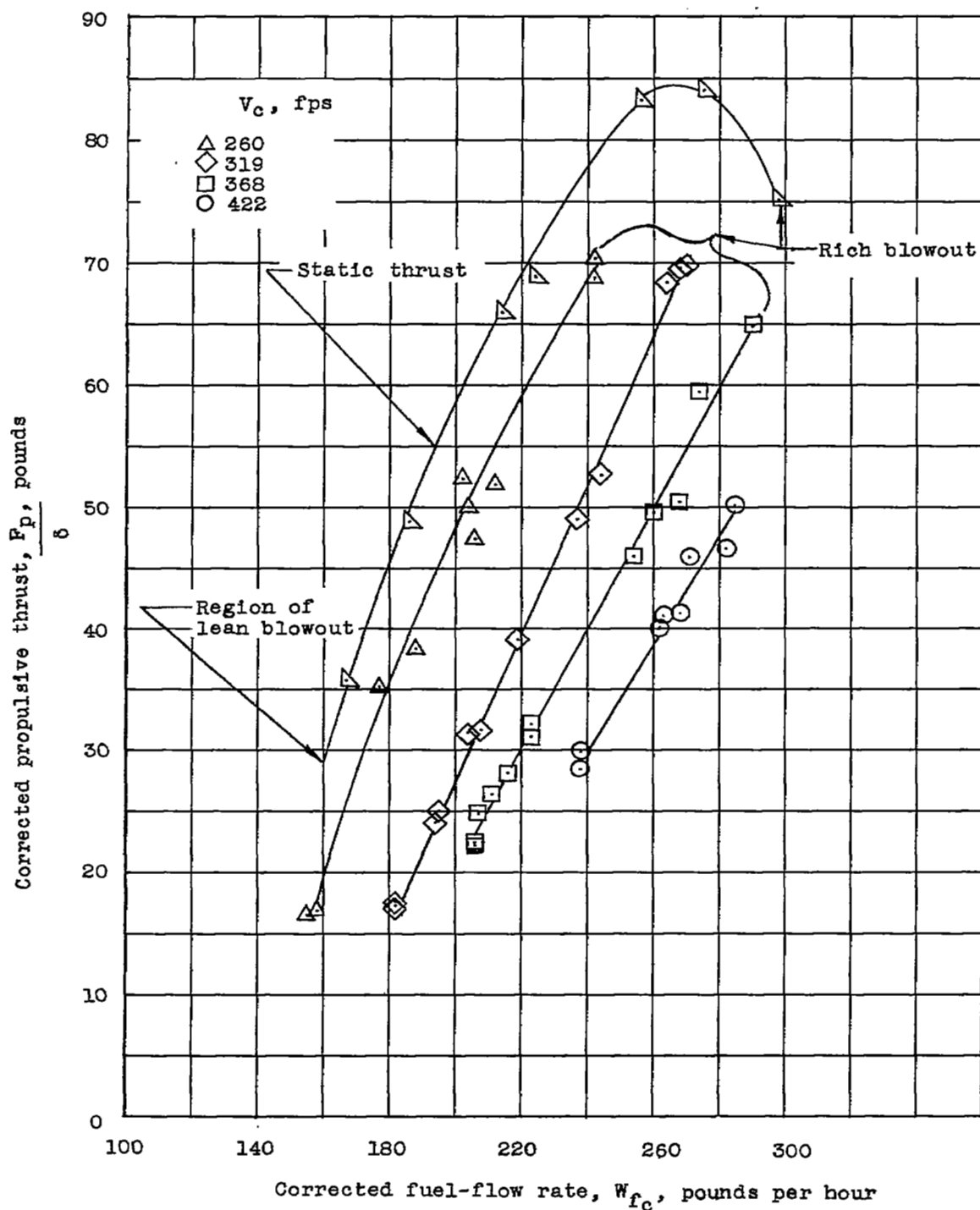


Figure 9.- Corrected pulse-jet propulsive thrust against corrected fuel consumption for one engine. Engine rigidly attached.

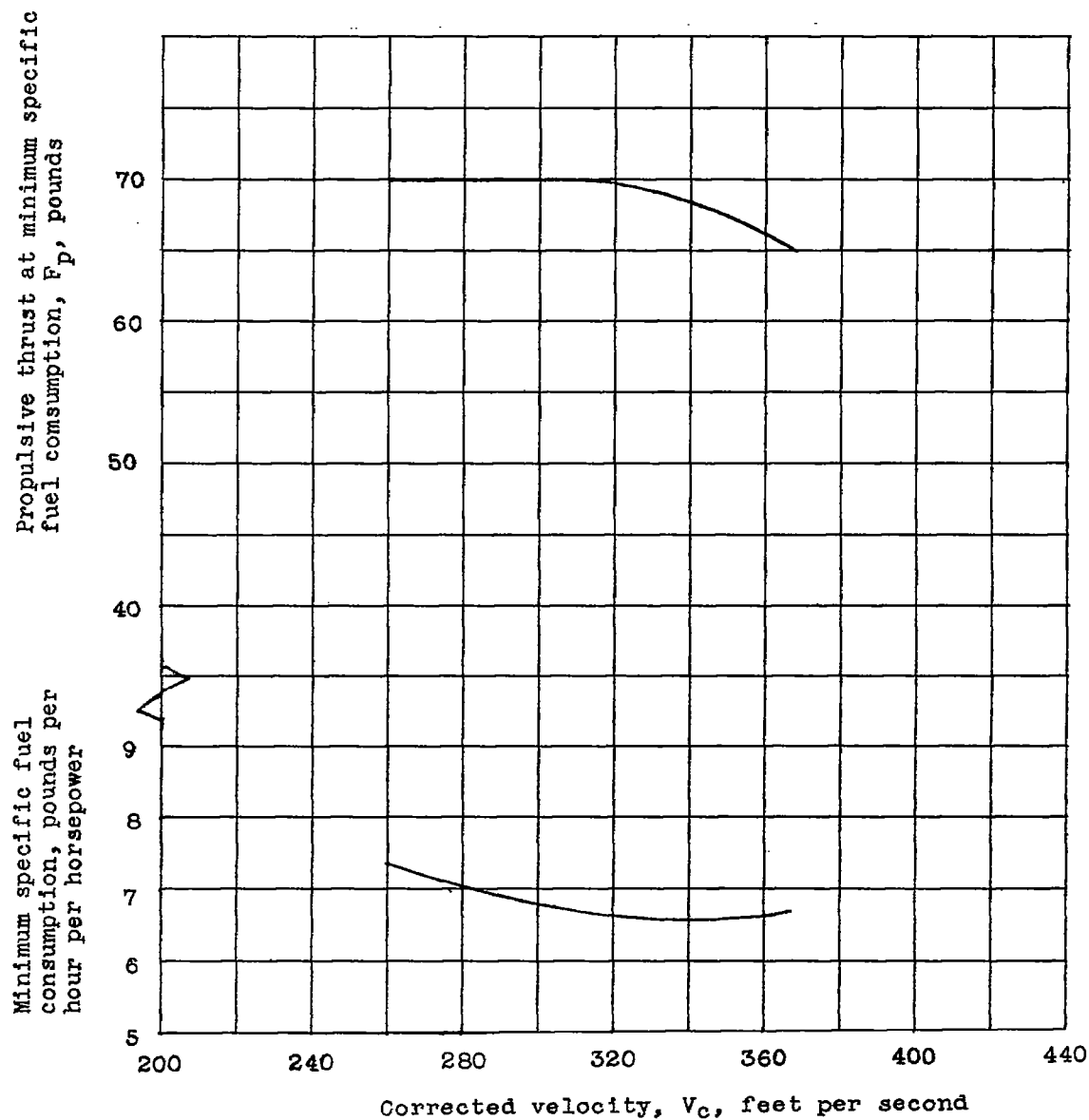


Figure 10.- Minimum specific fuel consumption and propulsive thrust at minimum specific fuel consumption for one engine as a function of corrected velocity. Engine rigidly attached.

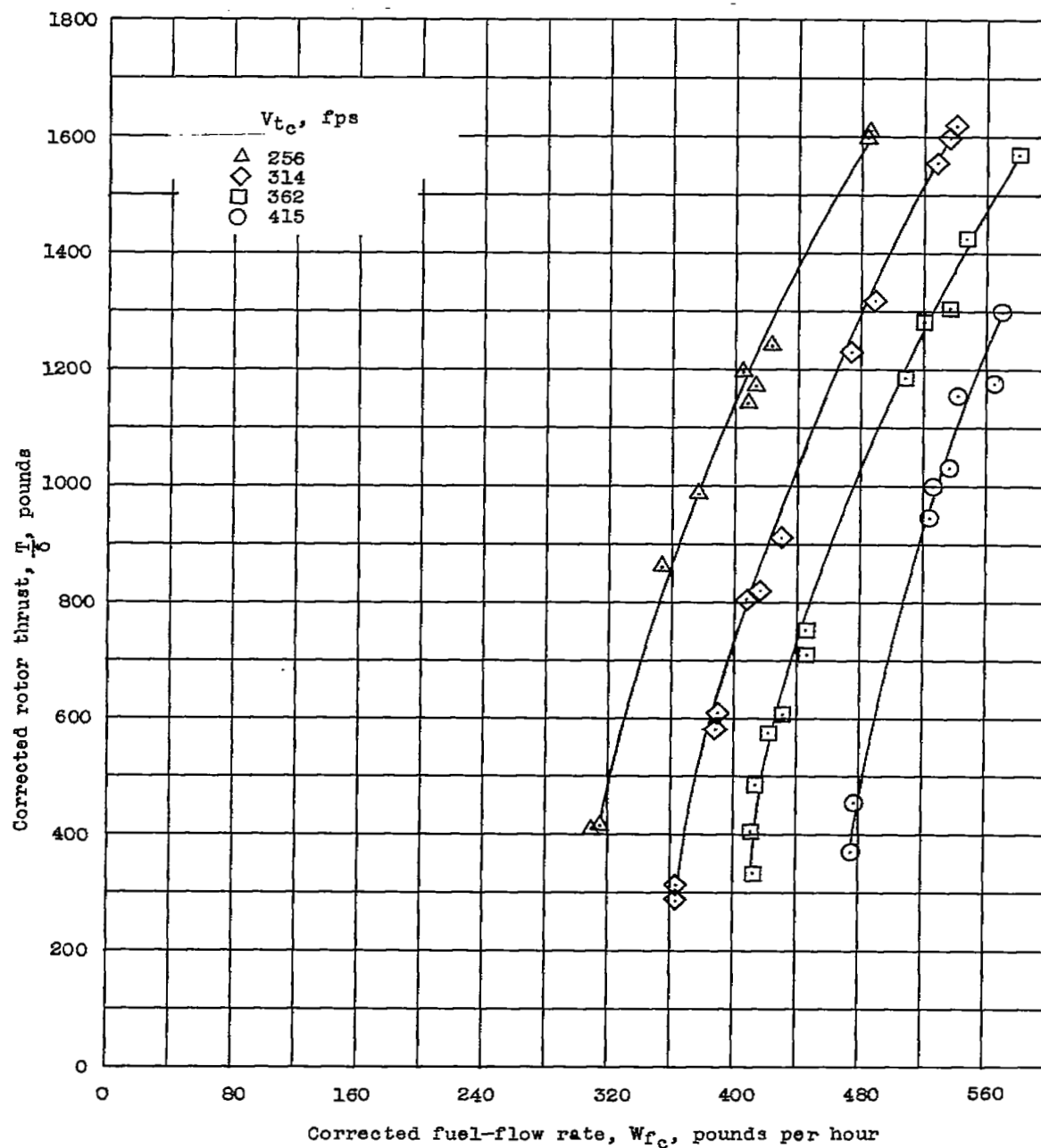


Figure 11.- Rotor thrust as a function of fuel-flow rate for various rotor tip speeds. Engines rigidly attached.

NASA Technical Library



3 1176 01437 6108

[REDACTED]